

# Ewald summation technique for interaction site models of polar fluids

IGOR P. OMEL'YAN

*Institute for Condensed Matter Physics, National Ukrainian Academy of Sciences  
1 Svientsitsky St., UA-290011 Lviv, Ukraine \**

## Abstract

A computer adapted fluctuation formula for the calculation of the wavevector- and frequency-dependent dielectric permittivity for interaction site models of polar fluids within the Ewald summation technique is proposed and applied to molecular dynamics simulations of the TIP4P water. The formula is analyzed and optimal parameters of the Ewald method are identified. A comparison of the obtained results with those evaluated within the reaction field approach is made.

*Keywords:* Computer simulation; Ewald technique; Dielectric properties

*PACS numbers:* 61.20.Ja; 77.22.-d; 24.60.-k

---

\*E-mail: nep@icmp.lviv.ua

# 1 Motivation

In order to achieve a macroscopic behaviour for investigated quantities in computer experiment based on the observation of finite systems, it is necessary to reduce the influence of surface effects to a minimum. This is especially important for polar systems with the long-range nature of interactions. Excluding the surface effects in simulations can be performed within either the reaction field (RF) [1–5] or Ewald summation [6–10] techniques. Now an equivalence between these techniques has been established for models of point dipoles and proper calculations can be made within either method [11, 12]. The explicit consideration of a finite-size medium lead to computer adapted fluctuation formulas [11–17] which allow one to calculate boundary free values for the dielectric constant on the basis of dipole moment fluctuations obtained in simulations. These formulas differ considerably with respect to those known from the theory of macroscopic systems even if the Ewald method is used [11]. Details of the summation must be taken into account explicitly in order to obtain correct values for the bulk dielectric constant.

Previously [18–20], the standard RF of point dipoles (PDRF) [3] has been applied to investigate more realistic, interaction site models (ISMs) [21] of polar fluids. The PDRF, however, being exact for point dipole models, may not be necessarily applicably to interpret simulation results for arbitrary systems [5]. Recently, it has been shown by actual calculations for a MCY water model that uncertainties for the dielectric quantities are significant if the PDRF is used in computer simulations of ISMs and an alternative scheme, the interaction site reaction field (ISRF) geometry, has been proposed [22]. At the same time, there is not such an approach concerning the entire wavevector and frequency dependence for the dielectric permittivity of ISMs within the Ewald geometry. The main attention of previous simulations [23–31] was directed to study the dielectric properties in the static limit or at zero and small wavevector values. Moreover, the macroscopic fluctuation formulas have been used in the simulation results without taking into account details of the Ewald summation.

In the present paper we apply the Ewald technique for treating Coulomb interactions in ISMs. The paper is organized as follows. A fluctuation formula suitable

for the calculation of the wavevector- and frequency-dependent dielectric constant is derived in Sec. 2 and optimal values of the Ewald parameters are determined there. The results of molecular dynamics simulations of the TIP4P water for time correlation functions related to dielectric polarization are presented in Sec. 3. These results are compared with those computed within the ISRF geometry. Concluding remarks are given in Sec. 4.

## 2 Ewald summation for ISMs

Consider a polar fluid with  $N$  molecules composed of  $M$  interaction sites which are confined in a volume  $V$ . The microscopic electric field created by the molecules at point  $\mathbf{r}$  and time  $t$  can be presented as  $\hat{\mathbf{E}}(\mathbf{r}, t) = \int_V \mathbf{D}(\mathbf{r} - \mathbf{r}') \hat{Q}(\mathbf{r}', t) d\mathbf{r}'$ , where  $\hat{Q}(\mathbf{r}, t) = \sum_{i=1}^N \sum_{a=1}^M q_a \delta(\mathbf{r} - \mathbf{r}_i^a(t))$  is the microscopic charge density,  $\mathbf{r}_i^a(t)$  and  $q_a$  denote the position and charge, respectively, of site  $a$  within the molecule  $i$  and  $\mathbf{D}(\boldsymbol{\rho}) = -\nabla 1/\rho$  is the operator of the Coulomb interactions.

Obviously, the field  $\hat{\mathbf{E}}(\mathbf{r}, t)$  for infinite systems ( $N, V \rightarrow \infty$ ) can not be reproduced exactly in computer experiment which deals with a finite, as a rule, cubic volume  $V = L^3$ , where  $L$  is the length of the simulation box edge. However, using the lattice summation, a macroscopic behaviour can be achieved considering the interactions between sites within the basic cell as well as an infinite lattice of its periodic images (the periodic boundary convention). This can be interpreted as an effective interaction which involves only the sites in the basic cell and characterized by a modified operator  $\mathcal{D}(\boldsymbol{\rho}) = \sum_{\mathbf{n}} \mathbf{D}(\boldsymbol{\rho} + \mathbf{n}L)$ , where the summation is extended over all vectors  $\mathbf{n}$  with integer components. It is more convenient to represent the lattice sum in a form, proposed by Ewald and Kornfeld (EK) [6], namely,  $\mathcal{D}(\boldsymbol{\rho}) = \mathbf{D}_1(\boldsymbol{\rho}) + \mathbf{D}_2(\boldsymbol{\rho})$ , where

$$\mathbf{D}_1(\boldsymbol{\rho}) = \sum_{0 \leq |\mathbf{n}| \leq \mathcal{N}} \mathbf{D}(\boldsymbol{\rho} + \mathbf{n}L) \left\{ \operatorname{erfc}(\eta|\boldsymbol{\rho} + \mathbf{n}L| + \frac{2\eta}{\sqrt{\pi}}|\boldsymbol{\rho} + \mathbf{n}L| \exp(-\eta^2|\boldsymbol{\rho} + \mathbf{n}L|^2)) \right\} \quad (1)$$

is a sum in real coordinate space, while

$$\mathbf{D}_2(\boldsymbol{\rho}) = \frac{1}{V} \sum_{0 < |\mathbf{k}| \leq k_{\max}} \mathbf{D}(\mathbf{k}) \exp(-k^2/4\eta^2 + i\mathbf{k} \cdot \boldsymbol{\rho}) \quad (2)$$

corresponds to summation over wavevectors  $\mathbf{k} = 2\pi\mathbf{n}/L$  of the reciprocal lattice space and  $\mathbf{D}(\mathbf{k}) = \int d\mathbf{r} e^{-i\mathbf{k}\cdot\boldsymbol{\rho}} \mathbf{D}(\boldsymbol{\rho}) = -4\pi i \mathbf{k}/k^2$  is the spatial Fourier transform of  $\mathbf{D}(\boldsymbol{\rho})$ . For the idealized summations ( $\mathcal{N} \rightarrow \infty, k_{\max} \rightarrow \infty$ ), the total sum of (1) and (2) is independent on the parameter  $\eta$ . The main advantage of the EK representation lies in the fact that values for  $\eta$  can be found in such a way that the both sums,  $\mathbf{D}_1$  and  $\mathbf{D}_2$ , converge very quickly and may be truncated after a finite number of terms. If the parameter  $\eta$  is chosen sufficiently large, we can restrict ourselves to a single term ( $\mathcal{N} = 0$ ) in the real space sum, corresponding to the basic cell to which toroidal boundary conditions are applied, and, additionally, to the spherical truncation  $|\boldsymbol{\rho}| \leq R$ , where  $R \leq L/2$ .

In such a case, taking the Fourier transforms of (1) and (2), after some algebra one obtains  $\mathbf{D}_1(\mathbf{k}) = -4\pi i D_1(k) \mathbf{k}/k^2$  and  $\mathbf{D}_2(\mathbf{k}) = -4\pi i D_2(k) \mathbf{k}/k^2$ , where

$$D_1(k) = \int_0^R k j_1(k\rho) \left( \operatorname{erfc}(\eta\rho) + \frac{2\eta}{\sqrt{\pi}} \rho \exp(-\eta^2 \rho^2) \right) d\rho, \quad (3)$$

$D_2(k) = \exp(-k^2/4\eta^2)$  if  $0 < k \leq k_{\max}$  and  $D_2(k) = 0$  otherwise and  $j_1(z) = \sin(z)/z^2 - \cos(z)/z$  denotes the spherical Bessel function of first order. Then the Fourier transform of the electric field is

$$\hat{\mathbf{E}}(\mathbf{k}, t) = \left( \mathbf{D}_1(\mathbf{k}) + \mathbf{D}_2(\mathbf{k}) \right) \hat{Q}(\mathbf{k}, t) = -4\pi \hat{\mathbf{P}}_L(\mathbf{k}, t) D(k), \quad (4)$$

where  $\hat{Q}(\mathbf{k}, t) = \sum_{i,a}^{N,M} q_a e^{-i\mathbf{k}\cdot\mathbf{r}_i^a(t)}$ ,  $\hat{\mathbf{P}}_L(\mathbf{k}, t) = \frac{i\mathbf{k}}{k^2} \hat{Q}(\mathbf{k}, t)$  is the longitudinal component of the microscopic operator  $\hat{\mathbf{P}}$  of polarization density ( $\nabla \cdot \hat{\mathbf{P}}(\mathbf{r}, t) = -\hat{Q}(\mathbf{r}, t)$ ) and  $D(k) = D_1(k) + D_2(k)$ .

Let us apply an external electric field  $\mathbf{E}_0(\mathbf{k}, \omega)$  to the system under consideration. The longitudinal, wavevector- and frequency-dependent dielectric constant is defined via the material relation  $4\pi \mathbf{P}_L(\mathbf{k}, \omega) = (\varepsilon_L(k, \omega) - 1) \mathbf{E}_L(\mathbf{k}, \omega)$ , where  $\mathbf{P}_L(\mathbf{k}, \omega) = \langle \hat{\mathbf{P}}_L(\mathbf{k}, \omega) \rangle$  and  $\mathbf{E}_L(\mathbf{k}, \omega) = \langle \hat{\mathbf{k}} \hat{\mathbf{k}} \cdot \mathbf{E}_0(\mathbf{k}, \omega) + \hat{\mathbf{E}}(\mathbf{k}, \omega) \rangle$  are macroscopic values for longitudinal components of the polarization and total field,  $\langle \rangle$  denotes statistical averaging at the presence of the external field and the time Fourier transform  $\mathcal{F}(\mathbf{k}, \omega) = \int_{-\infty}^{\infty} dt e^{-i\omega t} \mathcal{F}(\mathbf{k}, t)$  has been used for the functions  $\hat{\mathbf{P}}_L(\mathbf{k}, t)$ ,  $\hat{\mathbf{E}}(\mathbf{k}, t)$  and  $\hat{\mathbf{k}} = \mathbf{k}/k$ . Perturbation theory of the first order with respect to  $\mathbf{E}_0$

yields  $\mathbf{P}_L(\mathbf{k}, \omega) = -\frac{1}{V k_B T} \int_0^\infty dt e^{-i\omega t} \frac{d}{dt} \langle \hat{\mathbf{P}}_L(\mathbf{k}, 0) \cdot \hat{\mathbf{P}}_L(-\mathbf{k}, t) \rangle_0 \hat{\mathbf{k}} \hat{\mathbf{k}} \cdot \mathbf{E}_0(\mathbf{k}, \omega)$ , where  $\langle \rangle_0$  denotes equilibrium averaging at the absence of the external field, and  $k_B$  and  $T$  are the Boltzmann's constant and the temperature of the system, respectively. Then, eliminating  $\mathbf{E}_0(\mathbf{k}, \omega)$  from the presented above expressions, we obtain the desired fluctuation formula

$$\frac{\varepsilon_L(k, \omega) - 1}{\varepsilon_L(k, \omega)} = \frac{9y \mathcal{L}_{i\omega}(-\dot{G}_L(k, t))}{1 + 9y(1 - D(k)) \mathcal{L}_{i\omega}(-\dot{G}_L(k, t))} = 9y \mathcal{L}_{i\omega}(-\dot{g}_L(k, t)). \quad (5)$$

Here  $G_L(k, t) = \langle \hat{\mathbf{P}}_L(\mathbf{k}, 0) \cdot \hat{\mathbf{P}}_L(-\mathbf{k}, t) \rangle_0 / N\mu^2$  is the longitudinal component of the wavevector-dependent dynamical Kirkwood factor for the finite system,  $\mu = |\boldsymbol{\mu}_i|$  denotes the permanent magnitude of the molecule's dipole moment  $\boldsymbol{\mu}_i = \sum_a^M q_a \mathbf{r}_i^a$ ,  $y = 4\pi N\mu^2 / 9Vk_B T$  and  $\mathcal{L}_{i\omega}(\dots) = \int_0^\infty \dots e^{-i\omega t} dt$  is the Laplace transform. The right-hand side of Eq. (5) corresponds to the well-known fluctuation formula for infinite systems, where  $g_L(k, t) = \lim_{N \rightarrow \infty} G_L(k, t)$  is the infinite-system Kirkwood factor.

The computer adapted formula (5) reduces to the formula for infinite systems if the function  $D(k) = 1$ . It can be shown easily that for nonzero wavevectors the function  $D(k) \rightarrow 1$  if  $k_{\max} \rightarrow \infty$ , additionally provided  $\eta \rightarrow \infty$  at  $\mathcal{N} = 0$ . For  $k = 0$  the pattern is different because of finiteness of  $L$  and  $D(0) = 0$  as in the ISRF geometry [22]. However, in the case of an actual summation, when  $k_{\max}$  takes finite values, the factor  $D(k)$  can noticeably differ from unity. Therefore, the finite sample behaves like a macroscopic system if the function  $D(k)$  is very close to unity and this condition can be verified now quantitatively. Moreover, this explicit result may serve as an initial point for a more fruitful discussion about the Ewald method itself. Let  $\Delta = \max_k |1 - D(k)|$  be a maximal deviation of  $D(k)$  from unity in the whole interval of acceptable nonzero wavevector values for a chosen pair of parameters  $\eta$  and  $k_{\max}$ . Then an optimal value for  $\eta$  can be determined as that providing a global minimum for the function  $\Delta(\eta, k_{\max})$  at a given  $k_{\max}$ .

According to Eq. (5), the obtained in simulations Kirkwood factor  $G_L$  differs from its genuine value  $g_L$  with the relative precision of  $\chi = 9y\Delta$ . The function  $\chi(\eta, n_{\max})$  is shown in Fig. 1 as depending on  $\eta$  at fixed values of  $n_{\max} = k_{\max}L/2\pi$ . It has been calculated for the case of  $R = L/2$  and  $y = 5.47$  that corresponds to

the thermodynamics point  $\rho = mN/V = 1 \text{ g/cm}^3$ ,  $T = 293 \text{ K}$  of the TIP4P model, where  $m$  is the mass of water molecule. As we can see from the figure, the precision of calculations of dielectric quantities in computer experiment depends on Ewald parameters in a characteristic way. We indicate the existence of the sharp minimum of  $\chi$  at an arbitrary value of  $n_{\max}$ . The curves of Fig. 1 can be useful to estimate the possibility of a given simulation result to reproduce directly the macroscopic dielectric behaviour of an IS system in an arbitrary thermodynamics state, because then the function  $\chi' = \chi y'/y$  is simply rescaled, using the actual value of  $y'$ . From the last equality it follows that the precision of calculations is better for systems with lower particle densities  $N/V$ , molecular polarities  $\mu$  and higher temperatures  $T$ . It is obvious also that minimums of the functions  $\Delta$  and  $\chi$  with respect to Ewald parameters coincide between themselves.

The optimal pairs of values for  $\eta$  and  $n_{\max}$  at  $R = L/2$  as well as the corresponding values of the functions  $\Delta$  and  $\chi$  are selected in Table 1. Choosing a criterion  $\chi \lesssim 1\%$ , we may ask that the formula for infinite systems might be applied (at  $k \neq 0$ ) and the influence of summation details can be neglected in this case for which  $G_L(k, t)$  and  $g_L(k, t)$  are indistinguishable. It can be seen easily from the table that values of  $n_{\max} \geq 4$  satisfy this criterion if the parameter  $\eta$  is chosen optimally. The parameters  $n_{\max} = 5$ ,  $\eta L = 5.76$  and  $R = L/2$  are usually exploited in simulations [10]. For these values the relative precision is  $\chi = 0.22\%$ . However, choosing the optimal value  $\eta L = 5.929$  at  $n_{\max} = 5$  instead of  $\eta L = 5.76$ , we can reduce the uncertainty up to  $\chi = 0.13\%$ .

In the presented above consideration, the cut-off radius  $R$  has been putted to be half the basic cell length. Nevertheless, increasing  $n_{\max}$ , the same precision of summation can be achieved also at smaller values of  $R$ . Let  $\eta$  and  $n_{\max}$  correspond to the optimal parameters at  $R = L/2$ . And now we choose a smaller value of the cut-off radius in the form  $R' = R/l$ , where  $l > 1$ . Taking into account the fact that maximum deviations of  $D(k)$  from unity are always observed at  $k = 2\pi(n_{\max} + 1)/L$ , it is easy to show that the same value of  $\Delta(\eta, n_{\max})$  can be obtained also at  $\eta' = l\eta$  and  $n'_{\max} = l(n_{\max} + 1) - 1$ . For example, putting  $n_{\max} = 5$  and  $\eta L = 5.929$  at  $R = L/2$ , we then obtain for  $R = L/4$  ( $l = 2$ ) the following results:  $\eta' L = 11.858$  and

$n'_{\max} = 11$ . Choosing smaller values of  $R$  can be more convenient if the summation in  $\mathbf{k}$ -space takes less computation time in an actual programme than the summation in real space. Indeed, let  $t_1$  and  $t_2$  are the computation times in real and  $\mathbf{k}$ -space ( $t_1 > t_2$ ), respectively, at given values of  $R$  and  $n_{\max}$ . It is obvious that  $t_1 \sim R^3$  and  $t_2 \sim (n_{\max} + 1)^3$ . Then using new values  $n'_{\max} = l(n_{\max} + 1) - 1$  and  $R' = R/l$  and minimizing the total computation time  $t' = t'_1 + t'_2$  with respect to  $l$ , one obtains  $l = \sqrt[6]{t_1/t_2}$ . Therefore, in such a way we can provide even a time optimization of the programme without any loss of the precision.

### 3 Numerical results. Comparing the Ewald and reaction field methods

The study of dielectric properties by computer experiment is still a major challenge, given that the calculations are very sensitive to long-range interactions and because the polarization of polar fluids is a collective effect, so that long trajectories are required in order to obtain adequate statistical accuracy. For this reason, until now, the dynamical polarization of ISMs has been investigated at zero or small wavevector values only [18, 19, 23, 24, 27, 29, 31]. As far as we know, there are no computer experiment data on the entire wavevector dependence of dynamical dielectric quantities for such systems.

Our molecular dynamics simulations were carried out for the TIP4P model [32] in the microcanonical ensemble at a density of  $\rho = 1 \text{ g/cm}^3$  and at a temperature of  $T = 293 \text{ K}$ . We have performed two runs corresponding the Ewald and ISRF [22] geometries, respectively. In the both runs  $N = 256$  molecules were considered in the cubic sample  $V = L^3$  to which toroidal boundary conditions were applied ( $\mathcal{N} = 0$ ) and the interaction cut-off radius was half the basic cell length,  $R = L/2 = 9.856 \text{ \AA}$ . The simulations were started from a well equilibrated configuration for positions of sites, obtained by Monte Carlo simulations. Initial velocities of molecules were generated at random with the Maxwell distribution. The equations of motion were integrated with a time step of  $\Delta t = 2 \text{ fs}$  on the basis of a matrix method [33] using

the Verlet algorithm in velocity form. The system was allowed to achieve equilibrium for 50 000 time steps. The equilibrium state was observed during 500 000  $\Delta t = 1$  ns and each 10th time step was chosen to compute equilibrium averages. Translational and angular velocities of molecules were slightly rescaled after every 500 time steps in order to conserve the total energy of the system, so that the relative total energy fluctuations did not exceed 0.01% over the whole runs.

The dynamical Kirkwood factor was evaluated in the time interval of  $1000\Delta t = 2$  ps and in a very large wavenumber region, namely, at  $k = [0, 1, \dots, 300]k_{\min}$ , where  $k_{\min} = 2\pi/L = 0.319\text{\AA}^{-1}$ . Considering the system during such a rather long period of time allows us to achieve statistical accuracy for the investigated quantities of order 1%. The optimal parameters  $\eta L = 5.929$  and  $n_{\max} = 5$  have been used in the Ewald summation of Coulomb forces. The computational times on IBM PC AT486DX4 100 MHz to evaluate dynamics of the system in our Fortran programmes were 2.2 s and 1.2 s per step in the cases of Ewald and ISRF geometries, respectively.

Within the Ewald geometry the Coulomb part  $q_a q_b / |\boldsymbol{\rho}_{ij}^{ab}|$  of the intersite potential is replaced by

$$\varphi_{ij}^{ab} = q_a q_b \left\{ \Theta \left( R - |\bar{\boldsymbol{\rho}}_{ij}^{ab}| \right) \frac{\text{erfc}(\eta |\bar{\boldsymbol{\rho}}_{ij}^{ab}|)}{|\bar{\boldsymbol{\rho}}_{ij}^{ab}|} + \frac{4\pi}{V} \sum_{|\mathbf{k}| > 0}^{k_{\max}} \frac{e^{-\frac{k^2}{4\eta^2}}}{k^2} \cos(\mathbf{k} \cdot \boldsymbol{\rho}_{ij}^{ab}) \right\} = \varphi_1(|\bar{\boldsymbol{\rho}}_{ij}^{ab}|) + \varphi_2(\boldsymbol{\rho}_{ij}^{ab}). \quad (6)$$

Here,  $\boldsymbol{\rho}_{ij}^{ab} = \mathbf{r}_i^a - \mathbf{r}_j^b$  designates the distance between sites belonging the basic cell ( $\mathbf{r}_i^a, \mathbf{r}_j^b \in V$ ),  $\bar{\boldsymbol{\rho}}_{ij}^{ab} = \mathbf{r}_i^a - \bar{\mathbf{r}}_j^b$ , where, according to the toroidal boundary conditions,  $\bar{\mathbf{r}}_j^b = \mathbf{r}_j^b + \mathbf{p}L$  ( $\mathbf{p} = (p_x, p_y, p_z)$ ;  $p_x, p_y, p_z = 0, \pm 1$ ) is the position of the nearest image of  $\mathbf{r}_j^b$  with respect to  $\mathbf{r}_i^a$ , and  $\Theta$  denotes the Heviside function, i.e.,  $\Theta(\rho) = 1$  if  $\rho \geq 0$  and  $\Theta(\rho) = 0$  otherwise. The function  $\Theta$  indicates about the spherical site-site truncation in the real coordinate space. The force acting on the  $a$ -th charged site of molecule  $i$  due to the interaction with the  $b$ -th charge of molecule  $j$  is  $\mathbf{F}_{ij}^{ab} = -\partial\varphi_{ij}^{ab}/\partial\mathbf{r}_i^a$  or in a more explicit form

$$\begin{aligned} \mathbf{F}_{ij}^{ab} = q_a q_b \left\{ \frac{\bar{\boldsymbol{\rho}}_{ij}^{ab}}{|\bar{\boldsymbol{\rho}}_{ij}^{ab}|^3} \Theta \left( R - |\bar{\boldsymbol{\rho}}_{ij}^{ab}| \right) \left[ \text{erfc}(\eta |\bar{\boldsymbol{\rho}}_{ij}^{ab}|) + \frac{2\eta}{\sqrt{\pi}} |\bar{\boldsymbol{\rho}}_{ij}^{ab}| e^{-\eta^2 |\bar{\boldsymbol{\rho}}_{ij}^{ab}|^2} \right] \right. \\ \left. + \frac{4\pi}{V} \sum_{|\mathbf{k}| > 0}^{k_{\max}} \frac{\mathbf{k}}{k^2} e^{-\frac{k^2}{4\eta^2}} \sin(\mathbf{k} \cdot \boldsymbol{\rho}_{ij}^{ab}) \right\} \equiv q_a q_b \left( \mathbf{D}_1(|\bar{\boldsymbol{\rho}}_{ij}^{ab}|) + \mathbf{D}_2(\boldsymbol{\rho}_{ij}^{ab}) \right). \quad (7) \end{aligned}$$

We note that the  $\delta$ -like part  $q_a q_b \frac{\bar{\rho}_{ij}^{ab}}{R^2} \delta(R - |\bar{\rho}_{ij}^{ab}|) \text{erfc}(\eta R)$  of the force is not included in (7) for the reason that the complementary error function vanishes at  $|\rho_{ij}^{ab}| = R$  for sufficiently large values of  $\eta$ . In particular, in our case  $\text{erfc}(\eta R) = \text{erfc}(\eta L/2) = 0.0000276 \ll 1$ . Then the potential (6) can be considered as a continuous and continuously differentiable one and the drift of the total energy of the system, associated with the passage of sites through the surface of the truncation sphere, can be neglected.

In an actual molecular dynamics programme the current potential energy of the system,  $U = \frac{1}{2} \sum_{i \neq j}^N \sum_{a,b}^M \varphi_{ij}^{ab}$ , and the total force acting on the  $a$ -th site of molecule  $i$  due to interactions with all the rest of sites belonging other molecules,  $\mathbf{F}_i^a = \sum_{\substack{j=1 \\ (j \neq i)}}^N \sum_{b=1}^M \mathbf{F}_{ij}^{ab}$ , can be calculated as follows

$$U = \frac{1}{2} \left\{ \sum_{i \neq j}^N \sum_{a,b}^M \varphi_1(|\bar{\rho}_{ij}^{ab}|) + \frac{1}{\pi L} \sum_{|\mathbf{n}| > 0}^{n_{\max}} \frac{e^{-\frac{\pi^2 n^2}{\eta^2 L^2}}}{n^2} \mathcal{Y}(\mathbf{n}) \mathcal{Y}(-\mathbf{n}) - \sum_{i=1}^N \sum_{a,b}^M \varphi_2(\rho_{ii}^{ab}) \right\}, \quad (8)$$

$$\mathbf{F}_i^a = q_a \sum_{\substack{j=1 \\ (j \neq i)}}^N \sum_{b=1}^M q_b \mathbf{D}_1(|\bar{\rho}_{ij}^{ab}|) + \frac{2q_a}{L^2} \sum_{|\mathbf{n}| > 0}^{n_{\max}} \frac{\mathbf{n}}{n^2} e^{-\frac{\pi^2 n^2}{\eta^2 L^2}} i e^{-2\pi i \mathbf{n} \cdot \mathbf{r}_i^a / L} \mathcal{Y}(-\mathbf{n}) - q_a \sum_{b=1}^M q_b \mathbf{D}_2(\rho_{ii}^{ab}), \quad (9)$$

where the self electrostatic energy,  $u = \frac{1}{2} \sum_{i=1}^N \sum_{a \neq b}^M \varphi_{ii}^{ab}$ , and the self forces,  $\mathbf{f}_i^a = \sum_{\substack{b=1 \\ (b \neq a)}}^M \mathbf{F}_{ii}^{ab}$ , have been excluded from (8) and (9), respectively, because the intramolecular forces do not contribute into molecular translational accelerations and torques.

The auxiliary function

$$\mathcal{Y}(\mathbf{n}) = \sum_{i,a}^{N,M} q_a e^{-2\pi i \mathbf{n} \cdot \mathbf{r}_i^a / L} = \text{Re} \mathcal{Y}(\mathbf{n}) + i \text{Im} \mathcal{Y}(\mathbf{n}) \quad (10)$$

is introduced in order to reduce the total number of numerical operations in  $\mathbf{k}$ -space from of order  $(NM)^2 n_{\max}$  to  $NM n_{\max}$  that is very important for simulating large systems. This number can be reduced approximately twice yet, using invariance of the subsume expressions with respect to the inverse transformation  $\mathbf{n} \rightarrow -\mathbf{n}$ . Finally, taking into account that the real part of  $\mathcal{Y}(\mathbf{n})$  is an even function of  $\mathbf{n}$  and the imaginary part is an odd one, we obtain that only the real

part  $\text{Re} i e^{-2\pi i \mathbf{n} \cdot \mathbf{r}_i^a / L} \mathcal{Y}(-\mathbf{n}) = \sin(2\pi \mathbf{n} \cdot \mathbf{r}_i^a / L) \text{Re} \mathcal{Y}(\mathbf{n}) + \cos(2\pi \mathbf{n} \cdot \mathbf{r}_i^a / L) \text{Im} \mathcal{Y}(\mathbf{n})$  give nonzero contributions into (9) and  $\mathcal{Y}(\mathbf{n}) \mathcal{Y}(-\mathbf{n}) = (\text{Re} \mathcal{Y}(\mathbf{n}))^2 + (\text{Im} \mathcal{Y}(\mathbf{n}))^2$ .

In the RF geometry, real particles of the infinite system, which are located outside the sphere of finite radius  $R$  around a reference particle belonging to the basic cell, are replaced by an infinite, as a rule, conducting continuum. There are two versions of the RF geometry. In the PDRF approach, molecules are considered as point dipole particles and the intermolecular potential is of the form [18, 19]:

$$\varphi_{ij}^{\text{PD}} = \Theta(R - |\mathbf{r}_i - \bar{\mathbf{r}}_j|) \left( \sum_{a,b}^M \frac{q_a q_b}{|\bar{\boldsymbol{\rho}}_{ij}^{ab}|} - \frac{\boldsymbol{\mu}_i \cdot \boldsymbol{\mu}_j}{R^3} \right), \quad (11)$$

where  $\mathbf{r}_i$  is the centre of mass of the  $i$ -th molecule and the molecular cut-off is performed. In the exact ISRF method [22] the spatial distribution of charges within the molecule is taken into account explicitly at constructing the reaction field. As a result, the potential (11) transforms into

$$\varphi_{ij}^{\text{RF}} = \sum_{a,b}^M q_a q_b \Theta(R - |\bar{\boldsymbol{\rho}}_{ij}^{ab}|) \left\{ \frac{1}{|\bar{\boldsymbol{\rho}}_{ij}^{ab}|} + \frac{1}{2} \frac{|\bar{\boldsymbol{\rho}}_{ij}^{ab}|^2}{R^3} - \frac{3}{2R} \right\}, \quad (12)$$

where the first term in the right-hand side of (12) describes the usual Coulomb field, whereas the rest of terms corresponds to the reaction field in the IS description.

It can be shown easily that the potential (12) is reduced to (11) in one case only, namely, when  $d/R \rightarrow 0$ , where  $d = 2 \max_a |\mathbf{r}_i^a - \mathbf{r}_i|$  denotes the diameter of the molecule. In this case, the positions for sites and centres of mass are undistinguished within the same molecule. For finite samples of IS molecules we have  $d/R \neq 0$  and, therefore, the PDRF potential (11) may affect on a true macroscopic behaviour of the system considerably. Moreover, the ISRF method has yet a minor advantage over the PDRF scheme that the potential of interaction (12) is continuous and continuously differentiable. It is worth to mention also that in the RF geometry the dielectric permittivity is computed using the fluctuation formula (5) with the formal substitution  $D(k) \rightarrow D_{\text{RF}}(k) = 1 - 3j_1(kR)/(kR)$  [22].

The wavevector-dependent static Kirkwood factor,  $G_L(k) \equiv G_L(k, 0)$ , and samples of the normalized dynamical Kirkwood factor,  $\Phi_L(k, t) = G_L(k, t)/G_L(k)$ , calculated in the simulations within the Ewald and ISRF geometries, are shown in

Figs. 2, 3 by the circles and dashed curve, respectively. Since in the ISRF geometry the function  $D_{\text{RF}}(k)$  differs from unity considerably, to evaluate the infinite system Kirkwood factor  $g_{\text{L}}(k, t)$  the performance of the self-consistent transformation (5) is necessary. This result is plotted by the solid curve. At the same time, within the Ewald geometry the function  $D(k)$  is very close to unity at the given optimal parameters of summation (see Table 1), so that the infinite system Kirkwood factor is equivalent to that, obtained directly in the simulations, i.e.  $g_{\text{L}}(k, t) = G_{\text{L}}(k, t)$  (excepting the case  $k = 0$ ). As we can see from the figures, the agreement between the two sets of data for the infinite-system functions, corresponding to the Ewald and ISRF geometries, is quite good. The slight difference (within a few per cent) at large times can be explained by an approximate character of the integration appearing for the ISRF geometry at performing the inverse Laplace transform of (5).

For the purpose of comparison, the infinite-system Kirkwood factor  $g_{\text{L}}(k)$  corresponding to the PDRF geometry is also included in the Fig. 2 (the dotted curve). Deviations of values for  $g_{\text{L}}(k)$  obtained using the PDRF potential from those evaluated in the Ewald and ISRF geometries are of order 20%. They are well exhibited at intermediate values of wavevectors. Such a situation can be explained by the fact that the PDRF geometry does not take into account the spatial distribution of charges within the molecule and, thus, the precision of calculations for wavevector-dependent dielectric quantities at  $k \sim 2\pi/d \sim 3.4\text{\AA}^{-1}$  can not exceed  $d/R \sim 20\%$ , where  $d = 1.837\text{\AA}$  for the TIP4P water molecule. And only for great wavevector values ( $k > 6\text{\AA}^{-1}$ ), where the influence of boundary conditions is negligible ( $D_{\text{RF}}(k) \rightarrow 1$ ), all the three geometries become completely equivalent.

## 4 Conclusion

Explicitly considering details of the Ewald summation to treat Coulomb interactions, the fluctuation formula for the computation of the dielectric permittivity in IS models of polar fluids has been rigorously derived. Using this formula, it has been corroborated by actual molecular dynamics calculations that the Ewald and ISRF methods can be applied with equal successes to investigate the dielectric constant

of ISMs in computer experiment. The Ewald geometry, however, at a specific choice for parameters of the summation, may reproduce the macroscopic behaviour for dielectric quantities directly in simulations without any additional transformations.

Since the calculation of the wavevector- and frequency-dependent dielectric permittivity in simulations for ISMs is practical now in principle, we believe that this fact will stimulate further research of such systems in theory, computer and pure experiment.

**Acknowledgements.** The author would like to acknowledge financial support of the President of Ukraine.

## References

- [1] H. Frölich, Theory of Dielectrics (Clarendon Press, 1959).
- [2] C.J.F. Boettcher, Theory of Electric Polarization (Elsevier, 1973) Vol. 1.
- [3] J.A. Barker and R.O. Watts, Mol. Phys. 26 (1973) 789.
- [4] U.M. Titulaer and J.M. Deutch, J. Chem. Phys. 60 (1974) 1502.
- [5] H.L. Friedman, Mol. Phys. 29 (1975) 1533.
- [6] V.M. Jansoone, Chem. Phys. 3 (1974) 78.
- [7] D.J. Adams and I.R. McDonald, Mol. Phys. 32 (1976) 931.
- [8] S.W. De Leeuw, J.W. Perram and E.R. Smith, Proc. R. Soc. A 373 (1980) 27; 57.
- [9] M.P. Allen and D.J. Tildesley, Computer Simulation of Liquids (Clarendon Press, 1987).
- [10] D. Levesque, J.J. Weis and G.N. Patey, Mol. Phys. 51 (1984) 333.
- [11] M. Neumann and O. Steinhauser, Chem. Phys. Lett. 95 (1983) 417.
- [12] M. Neumann, Mol. Phys. 57 (1986) 97.
- [13] M. Neumann, Mol. Phys. 50 (1983) 841.
- [14] M. Neumann, O. Steinhauser and G.S. Pawley, Mol. Phys. 52 (1984) 97.
- [15] I.P. Omelyan, Phys. Lett. A 208 (1995) 237.
- [16] I.P. Omelyan, Mol. Phys. 87 (1996) 1273.
- [17] I.P. Omelyan, Phys. Lett. A 216 (1996) 211.

- [18] M. Neumann, *J. Chem. Phys.* 82 (1985) 5663.
- [19] M. Neumann, *J. Chem. Phys.* 85 (1986) 1567.
- [20] I.P. Omelyan, *Phys. Lett. A* 220 (1996) 167.
- [21] F.O. Raineri, H. Resat and H.L. Friedman, *J. Chem. Phys.* 96 (1992) 3068.
- [22] I.P. Omelyan, *Phys. Lett. A* 223 (1996) 295.
- [23] R.W. Impey, P.A. Madden and I.R. McDonald, *Mol. Phys.* 46 (1982) 513.
- [24] D.M.F. Edwards, P.A. Madden and I.R. McDonald, *Mol. Phys.* 51 (1984) 1141.
- [25] J. Anderson, J.J. Ullo and S. Yip, *J. Chem. Phys.* 87 (1987) 1726.
- [26] T. Fonseca and B.M. Ladanyi, *J. Chem. Phys.* 93 (1990) 8148.
- [27] M.S. Skaf, T. Fonseca and B.M. Ladanyi, *J. Chem. Phys.* 98 (1993) 8929.
- [28] M.S. Skaf and B.M. Ladanyi, *J. Chem. Phys.* 102 (1995) 6542.
- [29] B.M. Ladanyi and M.S. Skaf, *J. Phys. Chem.* 100 (1996) 1368.
- [30] P.A. Bopp, A.A. Kornyshev and G. Sutmann, *Phys. Rev. Lett.* 76 (1996) 1280.
- [31] D. Bertolini and A. Tani, *Mol. Phys.* 75 (1992) 1065.
- [32] W.L. Jorgensen, J. Chandrasekhar, J.D. Madura, R.W. Impey and M.L. Klein, *J. Chem. Phys.* 79 (1983) 926.
- [33] I.P. Omelyan, *Comput. Phys. Commun.* 109 (1998) 171.

**Table 1.** Optimal parameters of the Ewald summation for ISMs at  $R = L/2$

$\eta L$	$n_{\max}$	$\Delta(\%)$	$\chi(\%)$
3.301	1	1.632E+00	80.29
3.874	2	5.523E-01	27.17
4.791	3	6.684E-02	3.288
5.209	4	2.212E-02	1.088
5.929	5	2.690E-03	0.1324
6.276	6	8.978E-04	0.0442
6.887	7	1.094E-04	0.0054
7.251	8	3.602E-05	0.0018

### Figure captions

**Fig. 1.** The precision of reproducing bulk dielectric quantities in computer experiment for ISMs as depending on parameters of the Ewald geometry.

**Fig. 2.** The static wavevector-dependent Kirkwood factor of the TIP4P water. The obtained result in the Ewald geometry is presented by the full circles. The dashed and solid curves correspond to the finite and infinite systems in the ISRF geometry. The PDRF infinite-system Kirkwood factor is shown as the dotted curve.

**Fig. 3.** The normalized dynamical Kirkwood factor of the TIP4P water. Notations as for fig. 2.

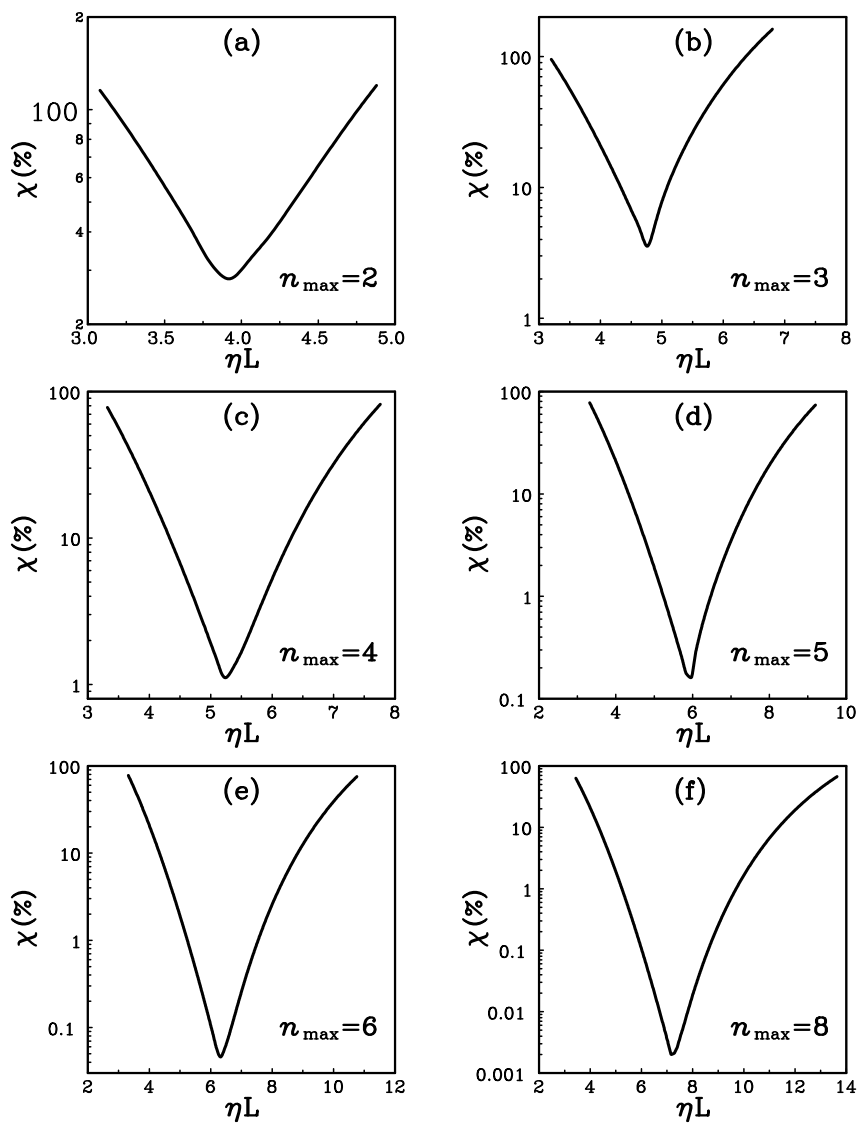
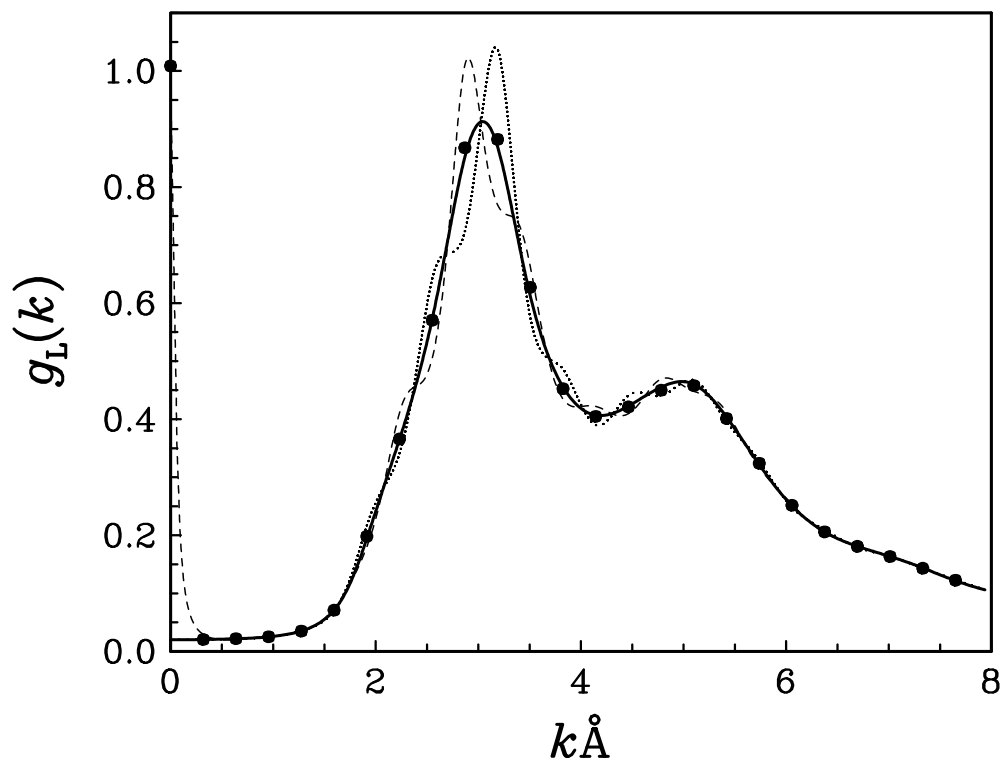


Fig. 1



*Fig. 2*

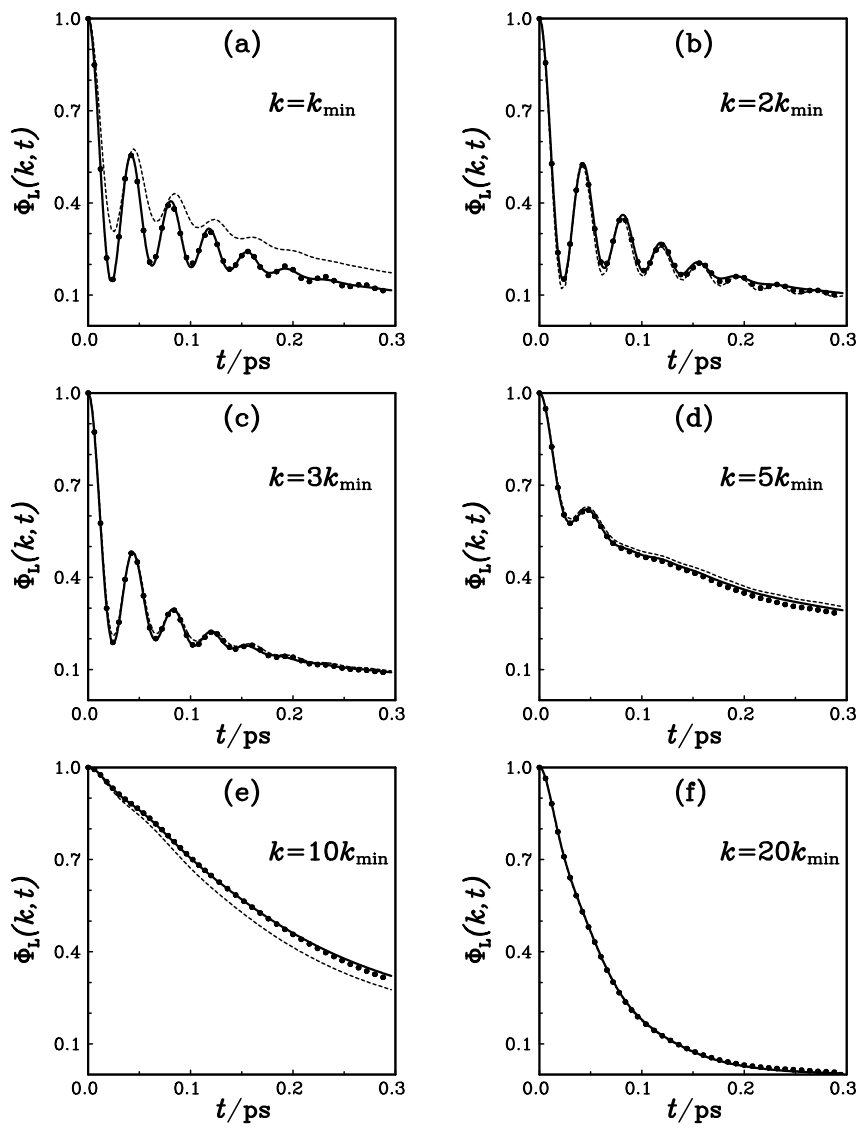


Fig. 3